Efficient removal of some anionic dyes from aqueous solution using a polymer-coated magnetic nano-adsorbent

Armin Kiani, Pouya Haratipour, Mazaher Ahmadi, Rouholah Zare-Dorabei and Ali Mahmoodi

ABSTRACT

For the efficient removal of some anionic dyes, a novel adsorbent was developed. The adsorbent was prepared by coating a synthetic polymer on magnetite nanosphere surface as a magnetic carrier. The synthesized nano-adsorbent was fully characterized using Fourier transform infrared spectroscopy (FT-IR), vibrating sample magnetometer, X-ray diffractometer, scanning electron microscope, and transmission electronic microscopy measurements. The synthesized nano-adsorbent showed high adsorption capacity towards removal of some anionic dyes (221.4, 201.6, and 135.3 mg g^{-1} for reactive red 195, reactive yellow 145, and reactive blue 19 dye, respectively) from aqueous samples. The dye adsorption was thoroughly studied from both kinetic and equilibrium points of view. It was found that the Langmuir isotherm showed a better correlation with the experimental data. The kinetic data showed that the process was very fast, and the adsorption process followed pseudo-second order kinetic models for the modified magnetic nano-adsorbent. Furthermore, the results showed that a stable and reusable (up to 20 cycles) nano-adsorbent for dye removal purposes was synthesized.

Key words | adsorption, anionic dyes, dye removal, magnetite nanospheres, polymeric adsorbent

Armin Kiani
Research Center for Analytical Chemistry,
KAVA Research Institute,
Tehran, Iran

Pouya Haratipour
Department of Chemistry,
Sharif University of Technology,
Tehran, Iran

Mazaher Ahmadi (corresponding author)
Young Researchers and Elite Club, Hamedan Branch,
Islamic Azad University,
Hamedan, Iran
E-mail: *m.ahmadi@iauh.ac.ir*

Rouholah Zare-Dorabei
Research Laboratory of Spectrometry & Micro/Nano Extraction, Department of Chemistry,
Iran University of Science and Technology,
Narmak, Tehran, Iran

Ali Mahmoodi
Department of Textile Engineering, Textile Engineering Faculty,
Isfahan University of Technology,
Isfahan, Iran

INTRODUCTION

The presence of organic contaminants in water causes some serious problems to aquatic life and human health disorders even in trace amounts (Chen & Wu 2014). Among various organic contaminants, discharge of synthetic dyes into the hydrosphere possess a significant source of pollution due to their recalcitrant nature. This gives an undesirable color to water bodies which will reduce sunlight penetration and disturbs photochemical and biological cycles of aquatic life (Wong *et al.* 2004). Synthetic dyes are widely used in many fields of advanced technology, e.g., in various kinds of the textile, paper, leather tanning, food processing, plastics, cosmetics, rubber, printing, and dye manufacturing industries. The release of synthetic dyes to the environment poses challenges to environmental scientists. These concerns have led to new and strict regulations concerning colored wastewater discharge as well as developing more efficient treatment technologies.

Various methods, such as adsorption, advanced oxidation processes, biodegradation, coagulation, and the membrane process, have been suggested to handle dye removal from water. All these processes have some advantages or disadvantages over the other methods (Khataee & Kasiri 2010; Chen & Wu 2014). A balanced approach is, therefore, needed to look into the worthiness on choosing an appropriate method which can be used to remove the dye in solution. The adsorption method is the most applied in the removal of organic dyes and pigments from wastewaters since it can produce high-quality water, and it can be employed as a process that is economically feasible (Madrakian *et al.* 2011). Many textile industries use

doi: 10.2166/aqua.2017.029

commercial activated carbon for the treatment of dye waste. Although activated carbon is commonly used as an adsorbent for color removal, its main disadvantage is its high production and treatment costs (Afkhami *et al.* 2007; Madrakian *et al.* 2011). Thus, many researchers throughout the world have focused their efforts on optimizing adsorption and developing novel alternative adsorbents with higher adsorption capacities and lower costs. In this regard, much attention has recently been paid to nanotechnology.

Nanometer-sized materials are widely used for the effective adsorption of different chemical species from water samples (Madrakian *et al.* 2013a; Kyzas & Matis 2015). The magnetic nanoparticle as an efficient adsorbent with a large specific surface area and small diffusion resistance has been recognized (Ngomsik *et al.* 2005). The magnetic separation provides a suitable route for online separation, where particles with affinity to target species are mixed with the heterogeneous solution. Upon mixing with the solution, the particles tag the target species. External magnetic fields are then applied to separate the tagged particles from the solution. Iron oxide nanoparticles (i.e., magnetite, maghemite, etc.) are attractive examples of magnetic nanoparticles. The synthesis of magnetite nanoparticles has been intensively developed not only for its high fundamental scientific interest but also for many technological applications in biology (Xie *et al.* 2004), medical applications (Ahmadi *et al.* 2015), bioseparation (Bucak *et al.* 2003); and separation and preconcentration of various anions and cations (Afkhami & Norooz-Asl 2009; Madrakian *et al.* 2012), due to their novel structural, electronic, magnetic, and catalytic properties. Recently, employing magnetite nanoparticles with modified surfaces has attracted the high attention of researchers for removal of cationic and anionic dyes from water (Ambashta & Sillanpää 2010; Madrakian *et al.* 2013c).

Herein, a novel magnetic adsorbent has been developed for dye removal and wastewater treatment purposes. In this regard, magnetite nanospheres were synthesized using the solvothermal method and further surface modification was performed using a synthetic polymer. The adsorbent was successfully utilized for removal of some anionic dyes (i.e., reactive yellow 145, reactive blue 19, and reactive red 195) from aqueous samples.

EXPERIMENTAL

Reagents and materials

Reactive yellow 145 (RY145), reactive blue 19 (RB19), and reactive red 195 (RR195) anionic dyes were purchased from Sigma-Aldrich Company (St Louis, MO, USA). Table 1 shows some chemical information of the investigated dyes. All of the other chemicals used were of analytical reagent grade and were purchased from Merck Company (Darmstadt, Germany). Double distilled water (DDW) was used throughout the work. The investigated dyes' stock solutions were prepared in DDW from their sodium salts and the working standard solutions of different dyes' concentrations were prepared daily by diluting the stock solution with DDW. Britton–Robinson (B-R) universal buffer was used for pH adjustment of the working solutions.

Apparatus

The size, morphology, and structure of the synthesized nanospheres were characterized by transmission electronic microscopy (TEM, Philips-CMC-300 KV) and scanning electron microscope (SEM, MIRA FEG-SEM, and TESCAN). The crystal structure of the synthesized nanospheres was determined by an X-ray diffractometer (XRD, 38066 Riva, d/G. via M. Misone, 11/D (TN) Italy) at ambient temperature. The magnetic properties of the synthesized nanospheres were measured using a vibrating sample magnetometer (VSM, 4 in. Daghigh Meghnatis Kashan Co., Kashan, Iran). The mid-infrared spectra of the synthesized nanospheres in the region of 4,000–400 cm^{-1} were recorded by a Fourier transform infrared spectrometer (FT-IR, Perkin-Elmer model Spectrum GX) using KBr pellets. A single beam ultraviolet (UV)-mini-WPA spectrophotometer was used for the determination of dye concentration in the solutions. A Metrohm model 713 pH meter was used for pH measurements. A 40 kHz universal ultrasonic cleaner water bath (RoHS, Korea) was used.

Synthesis of amidoamine monomer (AAM)

The AAM monomer was synthesized according to a previously reported procedure (Madrakian *et al.* 2013c).

Table 1 | Chemical information of the investigated anionic dyes

Name	Molecular formula	Molecular weight (g mol^{-1})	λ_{max} (nm)	Structure
RY145	$C_{28}H_{20}ClN_9Na_4O_{16}S_5$	1,026.25	421	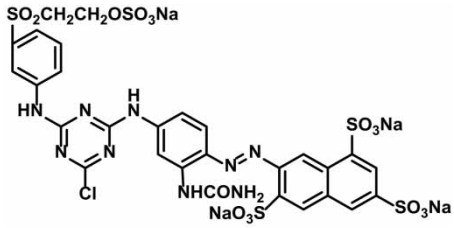
RB19	$C_{22}H_{16}N_2Na_2O_{11}S_3$	626.55	602	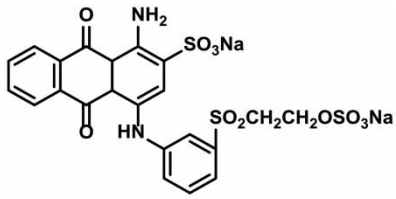
RR195	$C_{31}H_{19}ClN_7Na_5O_{19}S_6$	1,136.32	542	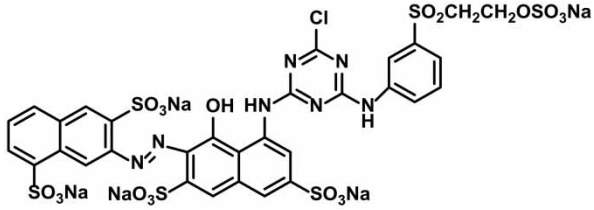

Briefly, the amidoamine monomer was synthesized by the slow addition of 1 g (0.01 mol) maleic anhydride to the solution of 1 mL (0.015 mol) ethylenediamine in 20 mL DDW. The solution was heated at 120°C for 1 h until all the water was removed and ethylenediamine reacted with maleic anhydride through ring opening (Figure 1(a)).

Synthesis of magnetite nanospheres (MNSs) and polymer-coated magnetite nanospheres (AMNSs)

MNSs were synthesized by the solvothermal reduction method with minor modifications (Deng *et al.* 2005). Typically, $FeCl_3.6H_2O$ (1.35 g) was dissolved in ethylene glycol (40.0 mL) to form a clear solution, followed by the addition of sodium acetate (3.6 g) and polyethylene glycol (1.0 g). The mixture was ultrasonicated vigorously for 30 min and then refluxed at 180°C for 8 h, and then allowed to cool down to room temperature. The black products were washed several times with ethanol and DDW water and then dried at 60°C for 6 h (Figure 1(b)).

In order to prepare the AMNSs, the amidoamine monomer was polymerized in the presence of MNSs (0.5 g, as the magnetic core), ammonium persulfate (0.1 g, as the initiator), and ethylene glycol dimethacrylate (50 μL, as the cross-linking monomer) in 30 mL DDW at 85°C for 12 h. Then, the product was separated using a magnet and washed with methanol and DDW to remove unreacted reagents.

Point of zero charge (pH_{PZC}) of AMNS nanospheres

The pH_{PZC} of the AMNSs was determined in degassed 0.01 mol L^{-1} $NaNO_3$ solution at room temperature. Aliquots of 30.0 mL 0.01 mol L^{-1} $NaNO_3$ were mixed with 0.03 g of the nanospheres in several beakers. The initial pH of the solutions was adjusted to 3.0, 4.0, 5.0, 6.0, 7.0, 8.0, 9.0, and 10.0 using 0.01 mol L^{-1} of HNO_3 and NaOH solutions as appropriate. The initial pHs of the solutions were recorded, and the beakers were covered with parafilm and shaken for 24 h. The final pH values were recorded and the differences between the initial and

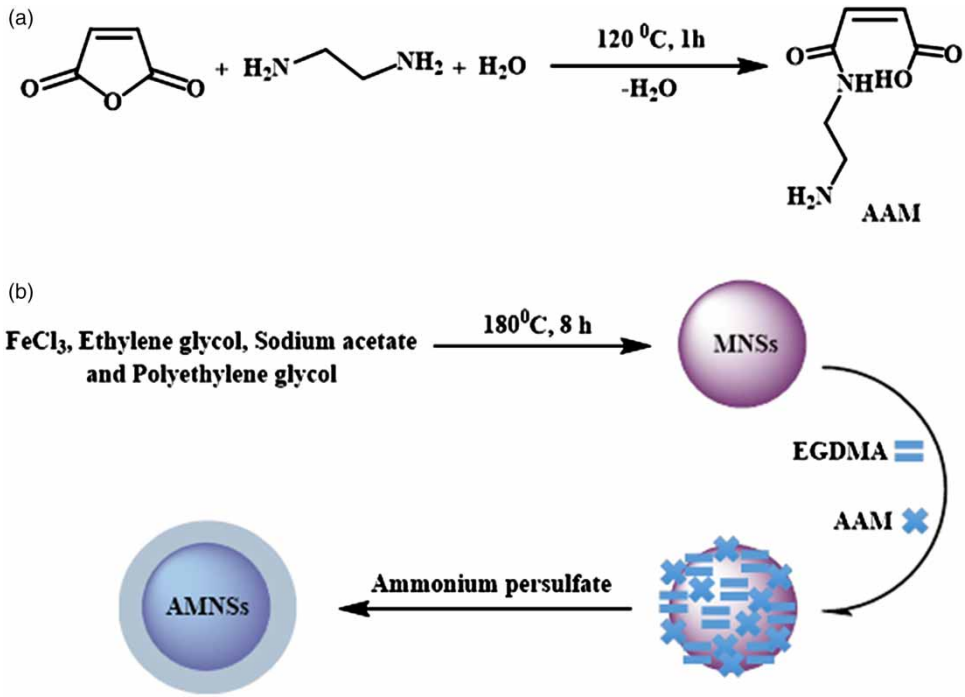

Figure 1 | Overall routes for the synthesis of (a) AAM monomer and (b) AMNS nanospheres.

final pH (ΔpH) of the solutions were plotted against their initial pH values. The pH_{PZC} corresponds to the pH where $\Delta pH = 0$ (Madrakian *et al.* 2013b). The pH_{PZC} for AMNSs was determined using the above procedure and was obtained as 6.7. The results are shown in Figure 2.

Dye removal experiments

Adsorption studies were performed by adding 0.02 g of AMNSs to 50.0 mL solution of 50 mg L^{-1} of dyes in a 100 mL beaker, and the pH of the solution was adjusted at 5.0 using a B-R pH buffer. The mixed solution was then shaken at room temperature for 20 min. Then, the dye loaded AMNSs were separated by magnetic decantation. The concentration of the dye in the solution was measured spectrophotometrically at the wavelength of the maximum absorbance of each dye (Table 1). The concentration of dyes decreased with time due to their adsorption by AMNSs. The adsorption percent for each dye, i.e., the dye removal efficiency, was determined using the following expression:

$$\%Re = \left[\frac{(C_0 - C_t)}{C_0}\right] \times 100 \quad (1)$$

where C_o and C_t represent the initial and final (after adsorption) concentration of dye in mg L^{-1}, respectively.

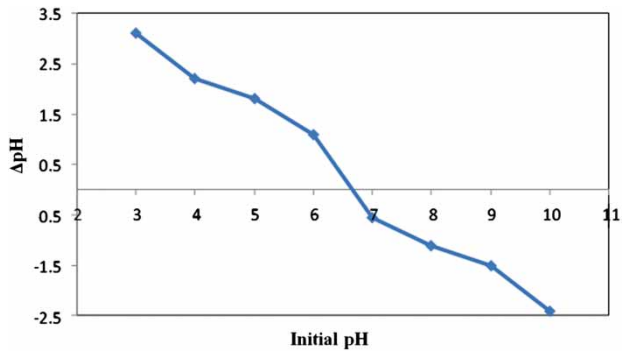

Figure 2 | Point of zero charge (pH_{PZC}) of AMNS nanospheres.

Adsorption kinetics

Adsorption is a physicochemical process that involves the mass transfer of a solute from the liquid phase to the adsorbent surface. The adsorption capacities of adsorbents were

calculated from the difference between the initial and the final concentration at any intermediate time. The sorption dynamics of the adsorption by AMNSs were tested with the pseudo-first order and the pseudo-second order kinetic models (Madrakian *et al.* 2013a).

To study the adsorption kinetics of the investigated dyes on AMNSs, 50.0 mg L^{-1} initial concentration of corresponding dye solutions which had been stirred in the presence of 0.02 g adsorbents at pH = 5.0 and for different time ranges (0–50 min) were used at room temperature. The solution was separated by magnetic decantation to remove adsorbent and analyzed spectrophotometrically.

Adsorption isotherms

The capacity of the adsorbent is an important factor that determines how much sorbent is required to remove quantitatively a specific amount of the dye from solution. For measuring the adsorption capacity of AMNSs, the absorbent was added into dye solutions at various concentrations (under optimum condition), and the suspensions were stirred at room temperature until the equilibrium was reached, followed by magnetic removal of the absorbent. An adsorption isotherm describes the fraction of the sorbate molecules that are partitioned between the liquid and the solid phase at equilibrium. Adsorption of the dyes by AMNS adsorbent was modeled using Freundlich (Freundlich & Heller 1939) and Langmuir (Langmuir 1916) adsorption isotherm models. The remaining dye in the supernatants was measured spectrophotometrically at the wavelength of the maximum absorbance of each dye, and the results were used to plot the isothermal adsorption curves.

Reusability and stability of the adsorbent

To evaluate the possibility of regeneration and the reuse of AMNS adsorbent, desorption experiments were performed. Dye desorption from the AMNSs was conducted by washing the dyes loaded on AMNSs using 2.0 mL of pure methanol, sodium hydroxide aqueous solution (0.1 M) and acetonitrile. For this purpose, 2.0 mL of eluent was added to 0.02 g of dye loaded AMNSs in a beaker. Then, the AMNSs were collected magnetically from the solution. The concentration of dyes in the desorbed solution was measured spectrophotometrically. Results showed that 0.1 M sodium hydroxide aqueous solution was an effective eluent for desorption of the dyes. It is notable that the equilibrium of desorption was achieved within about 10 min, which was fast, similar to the adsorption

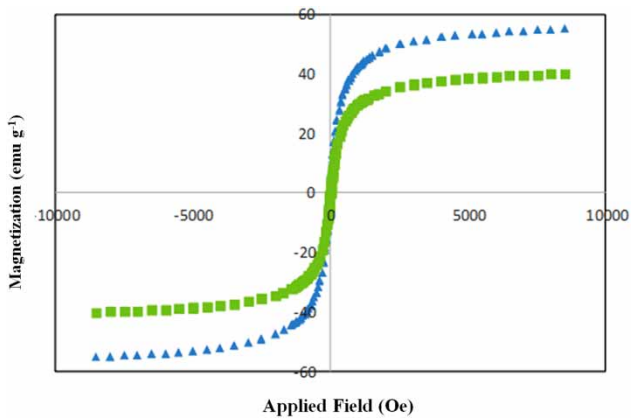

Figure 3 | Magnetization curves obtained by VSM at room temperature: (▲) bare MNS and (■) AMNS nanospheres.

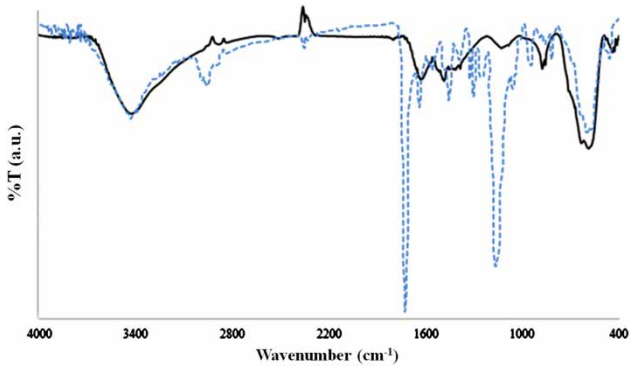

Figure 4 | The FT-IR spectra of (—) MNS and (---) AMNS nanospheres.

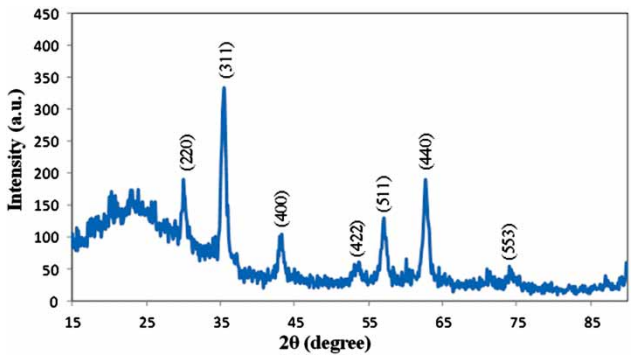

Figure 5 | XRD pattern of AMNS nanospheres.

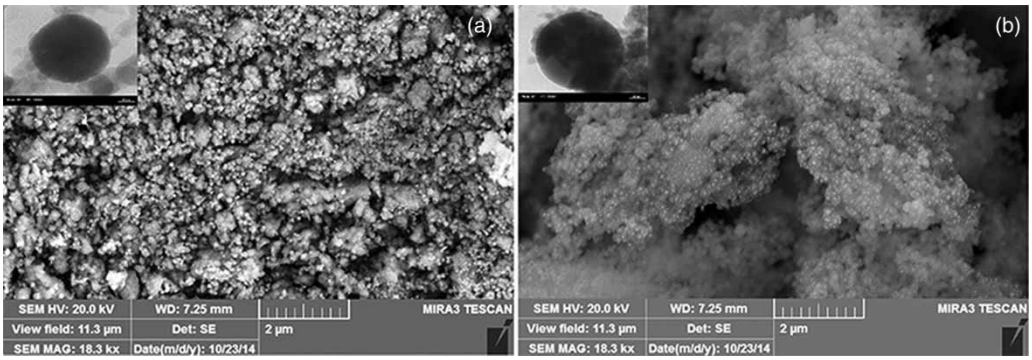

Figure 6 | SEM and TEM (insets) images of (a) MNS and (b) AMNS nanospheres.

equilibrium. This was due to the absence of internal diffusion resistance. After elution of the adsorbed dyes, the adsorbent was washed with DDW and vacuum dried at 50°C overnight and reused for the dye removal.

RESULTS AND DISCUSSION

The synthesized AMNSs were fully characterized using XRD, SEM, TEM, VSM, and FT-IR measurements. Then, batch experiments were used for evaluation and optimization affecting various parameters such as pH, contact time, and nanosphere dosage.

Characterization of the investigated nanospheres

The magnetization curves of the bare MNSs and AMNSs recorded with VSM are illustrated in Figure 3. As shown in Figure 3, the magnetization of the samples approach the saturation values when the applied magnetic field increases to 10,000 Oe. The saturation magnetizations of the MNSs and AMNSs were 55.20 and 40.05 emu/g, respectively. These results show that the AMNSs retain approximately 75% of the magnetization of the bare MNSs. A magnetization reduction of about 27.44% was observed between the bare MNSs and AMNSs. This may be related to the nanospheres' size effect, the increased surface disorder, and the diamagnetic contribution of the polymer layer.

The FT-IR spectra of the products were recorded to verify the formation of the expected products. The related spectra are shown in Figure 4. The characteristic absorption band of Fe-O in Fe_3O_4 (around 600 cm^{-1}) was observed in FT-IR spectra of MNSs and AMNSs. Two new absorption peaks at 1,730 cm^{-1} and 1,440 cm^{-1} in FT-IR spectra of AMNSs are assigned to C = O and C-N bands in the AMNSs, respectively. Moreover, new absorption peaks at 2,820 and 2,860 cm^{-1} are related to the stretching modes of aliphatic C-H bonds in the final product. Based on the above results, it can be concluded that the fabrication procedure was successfully performed.

The XRD pattern of AMNSs (Figure 5) shows diffraction peaks that are indexed to (2 2 0), (3 1 1), (4 0 0), (4 2 2), (5 1 1), (4 4 0), and (5 5 3) reflection characteristics of the cubic spinel phase of Fe_3O_4 (Joint Committee on Powder Diffraction Standards (JCPDS) powder diffraction data file no. 79–0418), revealing that the resultant nanospheres are mostly Fe_3O_4. The average crystallite size of the AMNSs was estimated to be 13 nm from the XRD data according to the Scherrer equation (Madrakian *et al.* 2013a).

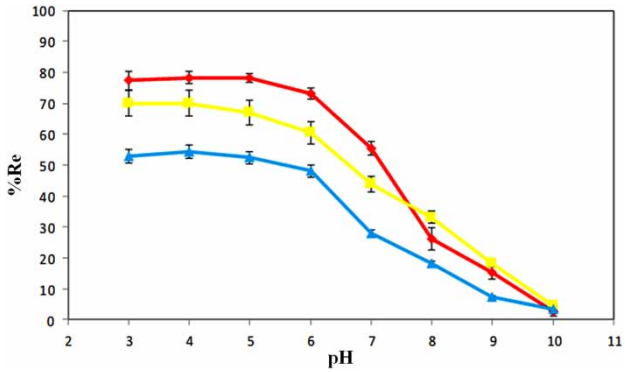

Figure 7 | Removal efficiencies of (♦) RR195, (▯) RY145, and (▲) RB19 at different pHs (conditions: 0.01 g of AMNSs, 50.0 mL of 50.0 mg L^{-1} of dyes, agitation time of 45 min, $N = 3$).

Table 2 | Adsorption kinetics parameters of the investigated dyes' adsorption on AMNSs

Kinetics models	Pseudo-second order				Pseudo-first order				
Dye	$q_{e,\,cal}$ (mg g^{-1})	$k_2 \times 10^{-3}$ (g mg^{-1} h^{-1})	R^2	RMS	$q_{e,\,cal}$ (mg g^{-1})	k_1 (h^{-1})	R^2	RMS	$q_{e,\,exp}$ (mg g^{-1})
RR195	191.16	0.61	0.996	1.32	146.01	0.025	0.974	3.21	192.30
RY145	134.56	1.24	0.989	1.05	107.54	0.153	0.961	2.85	133.34
RB19	72.18	1.05	0.987	2.10	57.91	0.127	0.909	3.64	75.79

The TEM and SEM images of the MNSs in Figure 6(a) indicate that spherical monodispersed nanoparticles with an average diameter of about 110 nm were synthesized. Figure 6(b) indicates that MNSs were successfully coated with a layer of the polymer. This figure shows that after the polymer layer coating process, thickness and morphological properties were, to some extent, changed.

Effect of pH

One of the important factors affecting the removal of the dyes from aqueous solutions is the pH of the solution. The dependence of dyes' molecules sorption on pH is related to both the dyes' chemistry in the solution and the ionization state of the functional groups of the sorbent which affects the availability of binding sites (Madrakian *et al.* 2011). All of the investigated dyes are anionic dyes. In the case of the adsorbent, the responsible parameter is the point of zero charge (pH_{PZC}). The point of zero charge is a characteristic of metal oxides (hydroxides) and is of fundamental importance in surface science. It is a concept relating to the phenomenon of adsorption and describes the condition when the electrical charge density on a surface is zero. The surface charge of AMNSs with primary amine groups (belong to the functional monomer) and hydroxyl groups (belong to MNSs) is largely dependent on the pH of the solution. The pH_{PZC} is caused by the amphoteric behavior of hydroxyl and surface amino groups, and the interaction between surface sites and the electrolyte species. When brought into contact with aqueous solutions, hydroxyl groups of surface sites can undergo protonation or deprotonation, depending on the solution pH, to form charged surface species.

The effect of pH on the dyes' removal efficiencies was investigated in the range of 3.0–10.0 using an initial dye concentration of 50.0 mg L^{-1} and a stirring time of 45 min, where the pH was adjusted with B-R buffer (Figure 7). Figure 7 indicates that the adsorbent provides the highest affinity to the dyes' molecules at pH 3–5. This is reasonable, because at this pH, the dyes are negatively charged and, on the other hand, the adsorbent surface charge at pH < 6.7 ($pH_{PZC} = 6.7$) is positive and electrostatic attraction force is responsible for the high dye removal efficiencies (Yagub *et al.* 2014).

Effect of nanosphere dosage

The dependence of the adsorption of the dyes on the modified nanospheres' amount was studied at room temperature and pH 5.0 by varying the adsorbent amount from 0.01 to 0.05 g in contact with 50.0 mL solution of 50.0 mg L^{-1} of the dyes with agitation time of 45 min. The results showed that increasing the amount of AMNSs increases the removal efficiencies of the dyes due to the availability of higher adsorption sites. The adsorption reached a maximum with 0.02 g of the adsorbent, and maximum percentage removal was about 98%.

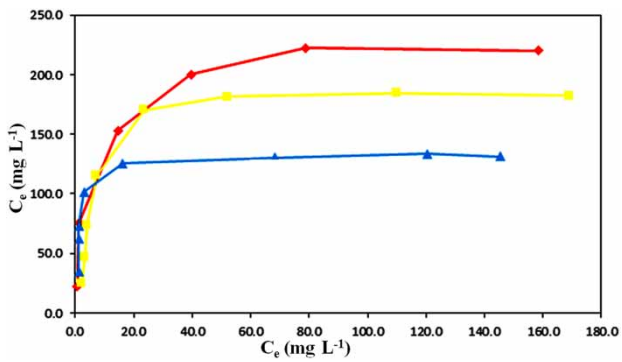

Figure 8 | Isothermal adsorption curves of (♦) RR195, (▬) RY145, and (▲) RB19 on AMNS adsorbent under optimum condition.

Table 3 | Adsorption isotherm parameters of Langmuir and Freundlich models for the adsorption of the dyes' molecules on AMNS adsorbent

	Langmuir				Freundlich			
Isotherm models	K_L (L mg^{-1})	q_{max} (mg g^{-1})	R^2	RMS	K_f	1/n	R^2	RMS
RR195	0.26	221.4	0.9927	0.97	70.27	0.25	0.8991	3.14
RY145	0.14	201.6	0.9968	1.14	55.25	0.26	0.7846	2.11
RB19	0.65	135.3	0.9944	1.08	66.89	0.15	0.8608	1.79

Adsorption kinetics

The removal of the dyes by adsorption on AMNSs was found to be rapid at the initial period (in the first ≈5th min) and then to become slow and stagnate with the increase in the contact time (≈5th to ≈15th min), and nearly reached a plateau after approximately the 20th min of the experiment. Different kinetic parameters of the dyes' adsorption onto AMNSs are shown in Table 2. All the experimental data showed better compliance with the pseudo-second order kinetic model regarding higher correlation coefficient value ($R^2 > 0.98$) and lower root mean square (RMS) value. Moreover, the q values ($q_{e,\ cal}$) calculated from the pseudo-second order model were more consistent with the experimental q values ($q_{e,\ exp}$) than with those calculated from the pseudo-first order model. Hence, it could be found that the pseudo-second order kinetic model was more valid to describe the adsorption behavior of the dyes onto AMNSs.

Adsorption isotherms

The isothermal adsorption curves are shown in Figure 8. The adsorption equilibrium data were fitted to Langmuir and Freundlich isotherm models by nonlinear regression. The resulting parameters are summarized in Table 2.

The higher correlation coefficient obtained for the Langmuir model, for all of the investigated dyes, and lower RMS values indicates that the experimental data are better fitted to this model, and adsorption of the investigated anionic dyes on AMNS adsorbent is more compatible with Langmuir assumptions, i.e., adsorption takes place at specific homogeneous sites within the adsorbent. The Langmuir model is based on the physical hypothesis that the maximum adsorption capacity consists of a monolayer adsorption, that there are no interactions between adsorbed molecules, and that the adsorption energy is distributed homogeneously over the entire coverage surface. This sorption model serves to estimate the maximum uptake values where they cannot be reached in the experiments.

According to the results (Table 3), the maximum amounts of the dyes that can be adsorbed by AMNSs were found to be 221.4, 201.6, and 135.3 mg g^{-1} at pH 5.0 in the case of RR195, RY145, and RB19, respectively. As the results show, the capacity factor for RR195 and RY145 is higher than that for RB19. The difference in capacity may be due to the difference in the structure of dyes and the number of the anionic functional groups.

Reusability and stability of the adsorbent

The reusability and stability of AMNSs for the removal of the investigated dyes were assessed by performing 25 consecutive separations/desorption cycles under the optimized conditions (Figure 9). The results showed that there was no significant change in the performance of the adsorbent

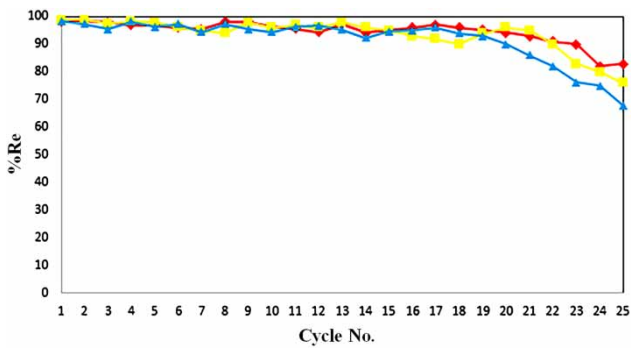

Figure 9 | The reusability and stability of AMNSs for the removal of 50.0 mL of 50.0 mg L^{-1} of (♦) RR195, (▼) RY145, and (▲) RB19 (conditions: AMNS dosage: 0.02 g, pH: 5, adsorption time: 45 min, eluent: 2 mL of 0.1 M sodium hydroxide solution, desorption time: 10 min).

Table 4 | Comparison of the calculated capacity factor for some synthetic adsorbents with the proposed one

	Capacity factor (mg g^{-1})			
Adsorbent	**RR195**	**RY145**	**RB19**	**Ref.**
Wheat bran	103.4	125.0	97.1	Çiçek *et al.* (2007)
P. oxalicum pellets	–	137	159	Zhang *et al.* (2003)
Chitosan flake	–	188	–	Wu *et al.* (2001)
Nano-MgO	–	–	166.7	Moussavi & Mahmoudi (2009)
Magnetic nanoparticle/ polyethyleneimine	–	–	121	Liao *et al.* (2006)
AMNSs	221.4	201.6	135.3	This work

during the first 20 cycles, indicating that the fabricated adsorbent is a reusable solid phase adsorbent for the removal of the investigated dyes during these 20 cycles. Furthermore, the results showed that the efficiencies of the recycled adsorbent for removing the investigated dyes are nearly the same as those for the fresh ones even after 20 times recycling. The removal efficiencies decreasing at higher cycles might be due to washing the polymer from the magnetic nanospheres during the adsorbent regeneration process. To evaluate this theory, the bare MNSs were used for the removal of the same concentration of the investigated dyes under the optimized conditions. The results showed that only 20.6, 18.2, and 12.4% of RR195, RY145, and RB19 could be removed using the bare MNSs at the first cycle, and confirming the critical role of the coated polymer to increase the adsorption capacity of the AMNSs toward the investigated dyes.

In Table 4, we compared the ability of our inexpensive adsorbent with other adsorbents in the removal of the dyes from aqueous solutions. The results show that AMNSs are a better adsorbent compared to some of the adsorbents.

CONCLUSION

In this work, a magnetic adsorbent was developed for dye removal purposes. The prepared magnetic adsorbent is well dispersed in the water medium and be easily separated magnetically from the medium after the dyes' adsorption process. The rapid adsorption rate is mainly attributed to the polymer structure and functional groups on the adsorbent providing a large surface area and good affinity for the facile and fast adsorption of dye molecules. The Langmuir isotherm model well fitted the adsorption data. As the calculated capacity factors of AMNSs show, they are a very good adsorbent for removing the investigated anionic dyes. The results of this study suggest that the developed adsorbent can be considered as an alternative adsorbent for wastewater treatments and controlling environmental pollution.

ACKNOWLEDGEMENTS

The authors gratefully acknowledge the financial support provided by Centre for Analytical Chemistry-KAVA Research Institute (CAC-KRI, Project No. Y34CS024/2013). The authors also acknowledge the Research Laboratory of Spectrometry & Micro/Nano Extraction of Iran University of Science and Technology (RLSMNE-IUST) for their support.

REFERENCES

Afkhami, A. & Norooz-Asl, R. 2009 Removal, preconcentration and determination of Mo(VI) from water and wastewater samples using maghemite nanoparticles. *Colloids and Surfaces A: Physicochemical and Engineering Aspects* **346**, 52–57.

Afkhami, A., Madrakian, T., Karimi, Z. & Amini, A. 2007 Effect of treatment of carbon cloth with sodium hydroxide solution on its adsorption capacity for the adsorption of some cations. *Colloids and Surfaces A: Physicochemical and Engineering Aspects* **304**, 36–40.

Ahmadi, M., Madrakian, T. & Afkhami, A. 2015 Solid phase extraction of doxorubicin using molecularly imprinted polymer coated magnetite nanospheres prior to its spectrofluorometric determination. *New Journal of Chemistry* **39**, 163–171.

Ambashta, R. D. & Sillanpää, M. 2010 Water purification using magnetic assistance: a review. *Journal of Hazardous Materials* **180**, 38–49.

Bucak, S., Jones, D. A., Laibinis, P. E. & Hatton, T. A. 2003 Protein separations using colloidal magnetic nanoparticles. *Biotechnology Progress* **19**, 477–484.

Chen, Q. & Wu, Q. 2014 Preparation of carbon microspheres decorated with silver nanoparticles and their ability to remove dyes from aqueous solution. *Journal of Hazardous Materials* **283**, 193–201.

Çiçek, F., Özer, D., Özer, A. & Özer, A. 2007 Low cost removal of reactive dyes using wheat bran. *Journal of Hazardous Materials* **146**, 408–416.

Deng, H., Li, X., Peng, Q., Wang, X., Chen, J. & Li, Y. 2005 Monodisperse magnetic single-crystal ferrite microspheres. *Angewandte Chemie International Edition* **44**, 2782–2785.

Freundlich, H. & Heller, W. 1939 The adsorption of cis- and trans-azobenzene. *Journal of the American Chemical Society* **61**, 2228–2230.

Khataee, A. R. & Kasiri, M. B. 2010 Photocatalytic degradation of organic dyes in the presence of nanostructured titanium dioxide: influence of the chemical structure of dyes. *Journal of Molecular Catalysis A: Chemical* **328**, 8–26.

Kyzas, G. Z. & Matis, K. A. 2015 Nanoadsorbents for pollutants removal: a review. *Journal of Molecular Liquids* **203**, 159–168.

Langmuir, I. 1916 The constitution and fundamental properties of solids and liquids. Part I. Solids. *Journal of the American Chemical Society* **38**, 2221–2295.

Liao, M.-H., Chen, W.-C. & Lai, W.-C. 2006 Magnetic nanoparticles assisted low-molecular weight polyethyleneimine for fast and effective removal of reactive blue 19. *Fresenius Environmental Bulletin* **15**, 609–613.

Madrakian, T., Afkhami, A., Ahmadi, M. & Bagheri, H. 2011 Removal of some cationic dyes from aqueous solutions using magnetic-modified multi-walled carbon nanotubes. *Journal of Hazardous Materials* **196**, 109–114.

Madrakian, T., Afkhami, A., Zolfigol, M., Ahmadi, M. & Koukabi, N. 2012 Application of modified silica coated magnetite nanoparticles for removal of iodine from water samples. *Nano-Micro Letters* **4**, 57–63.

Madrakian, T., Afkhami, A. & Ahmadi, M. 2013a Simple in situ functionalizing magnetite nanoparticles by reactive blue-19 and their application to the effective removal of Pb^{2+} ions from water samples. *Chemosphere* **90**, 542–547.

Madrakian, T., Afkhami, A., Mahmood-Kashani, H. & Ahmadi, M. 2013b Superparamagnetic surface molecularly imprinted nanoparticles for sensitive solid-phase extraction of tramadol from urine samples. *Talanta* **105**, 255–261.

Madrakian, T., Ahmadi, M., Afkhami, A. & Soleimani, M. 2013c Selective solid-phase extraction of naproxen drug from human urine samples using molecularly imprinted polymer-coated magnetic multi-walled carbon nanotubes prior to its spectrofluorometric determination. *Analyst* **138**, 4542–4549.

Moussavi, G. & Mahmoudi, M. 2009 Removal of azo and anthraquinone reactive dyes from industrial wastewaters using MgO nanoparticles. *Journal of Hazardous Materials* **168**, 806–812.

Ngomsik, A.-F., Bee, A., Draye, M., Cote, G. & Cabuil, V. 2005 Magnetic nano- and microparticles for metal removal and environmental applications: a review. *Comptes Rendus Chimie* **8**, 963–970.

Wong, Y. C., Szeto, Y. S., Cheung, W. H. & McKay, G. 2004 Adsorption of acid dyes on chitosan–equilibrium isotherm analyses. *Process Biochemistry* **39**, 695–704.

Wu, F.-C., Tseng, R.-L. & Juang, R.-S. 2001 Enhanced abilities of highly swollen chitosan beads for color removal and tyrosinase immobilization. *Journal of Hazardous Materials* **81**, 167–177.

Xie, X., Zhang, X., Yu, B., Gao, H., Zhang, H. & Fei, W. 2004 Rapid extraction of genomic DNA from saliva for HLA typing on microarray based on magnetic nanobeads. *Journal of Magnetism and Magnetic Materials* **280**, 164–168.

Yagub, M. T., Sen, T. K., Afroze, S. & Ang, H. M. 2014 Dye and its removal from aqueous solution by adsorption: a review. *Advances in Colloid and Interface Science* **209**, 172–184.

Zhang, S. J., Yang, M., Yang, Q. X., Zhang, Y., Xin, B. P. & Pan, F. 2003 Biosorption of reactive dyes by the mycelium pellets of a new isolate of Penicillium oxalicum. *Biotechnology Letters* **25**, 1479–1482.

First received 22 April 2016; accepted in revised form 23 December 2016. Available online 7 April 2017